Electronic Supplementary Information for

Oximes as Reversible Links in Polymer Chemistry: Dynamic Macromolecular Stars

Soma Mukherjee, Abhijeet P. Bapat, Megan R. Hill and Brent S. Sumerlin*

George & Josephine Butler Polymer Research Laboratory, Center for Macromolecular Science & Engineering, Department of Chemistry, University of Florida, Gainesville, FL 32611, USA

E-Mail: sumerlin@chem.ufl.edu

Experimental

Materials.
2–Dodecylsulfanylthiocarbonylsulfanyl–2–methyl–propionic acid (DMP) was prepared as previously reported.[1] *N,N*–Dimethylacrylamide (DMA, Fluka, 98%) was passed through a small column of basic alumina to remove inhibitor prior to polymerization. Diacetone acrylamide (DAA, 99%, Sigma Aldrich) was recrystallized from hexane. 2,2′–Azobisisobutyronitrile (AIBN, Sigma Aldrich, 98%) was recrystallized from ethanol. *O*–(Tetrahydro–2*H*–pyran–2–yl)hydroxylamine (Sigma Aldrich, 96%), *O*–allyl hydroxylamine hydrochloride (≥98.0%, Fluka), *O,O′*–1,3–propanediylbishydroxylamine dihydrochloride (Sigma Aldrich, >99%), acryloyl chloride (Alfa Aesar, 96%), 4–hydroxy–2–butanone (Alfa Aesar, 95%), trifluroacetic acid (TFA, 99.5%, EMD Millipore), triethyl amine (TEA, Fisher Chemical, 99%), 1,3,5–trioxane (Acros Organics, 99.5%), sodium hydrogen carbonate (Acros Organics, 99.5%), *N,N*–dimethylformamide (DMF, EMD, 99.9%), dimethyl acetamide (DMAc, Sigma Aldrich, 99.9%), tetrahydrofuran (THF, EMD, 99.5%), dichloromethane (DCM, 99.5%, BDH), 1,4–dioxane (Fisher Chemicals, 99%), phosphate buffered saline (PBS, pH 7.4, Sigma Aldrich), diethyl ether (Fisher Chemicals), methanol (Mallinckrodt), ethyl acetate (99.9%, Fisher chemicals), hexane (98.5%, BDH), dimethylsulfoxide–d_6 (DMSO-d_6, Cambridge Isotope, 99.9% D), $CDCl_3$ (Cambridge Isotope, 99% D), and molecular sieves 4Å (Acros Organics) were used as received.

Instrumentation and Analysis. Molecular weight and molecular weight dispersity were determined by size exclusion chromatography (SEC). (i) SEC in DMF (with 0.05 M LiBr) was conducted at 55 °C with a flow rate of 1.0 mL/min (Viscotek SEC Pump; Columns [(ViscoGel I-Series G3000 and G4000 mixed bed columns: molecular weight range 0–60 x 10^3 and 0–400 x 10^3 g/mol, respectively), or (Polymer Laboratories; PolarGel-M mixed bed columns: molecular weight range 0–60 x 10^3 and 0–2000 x 10^3 g/mol)]. Detection consisted of a Viscotek refractive index detector operating at λ = 660 nm, a Viscotek UV-Vis detector operating at λ = 254 nm, and a Viscotek Model 270 series platform, consisting of a laser light scattering detector (operating at 3 mW, λ = 670 nm with detection angles of 7 and 90 °) and a four capillary viscometer. Molecular weights were determined by the triple detection method assuming 100% mass recovery. (ii) SEC in DMAc with 0.05 M LiCl at 55 °C and a flow rate of 1.0 mL/min (Viscotek SEC pump, columns: Guard + two ViscoGel I-series G3078 mixed bed columns: molecular weight range 0–20 × 10^3 and 0–100 × 10^4 g/mol; or Agilent isocratic pump, degasser, and autosampler, columns: PLgel 5 µm guard + two ViscoGel I-series G3078 mixed bed columns: molecular weight range 0–20 × 10^3 and 0–100 × 10^4 g/mol). Detection either consisted of a Viscotek VE 3580 refractive index detector operating at 660 nm, or a Wyatt Optilab T-rEX refractive index detector operating at 658 nm and a Wyatt miniDAWN TREOS light scattering detector operating at 659 nm. Molecular weights were determined using narrowly dispersed polystyrene standards for column calibration. Absolute molecular weights and molecular weight dispersities were calculated using the Wyatt ASTRA software. Dynamic light scattering (DLS) was conducted at 173° with a Malvern Zetasizer Nano–ZS equipped with a 4 mW, 633 nm He–Ne laser and an Avalanche photodiode detector. UV-Vis spectroscopic measurements were conducted with Varian Cary 500 Scan UV-Vis NIR spectrophotometer. ^{1}H NMR spectra were recorded using JEOL Delta 500 or Inova spectrometers operating at 500 MHz. Chemical shifts are reported in parts per million (ppm) downfield relative to tetramethylsilane (TMS, 0.0 ppm). Multiplicities are reported using the following abbreviations: s, singlet; d, doublet; t, triplet; q, quartet; m, multiplet; br, broad. Transmission electron microscopy (TEM) images were taken on an H-7000 TEM microscope (Hitachi, Japan) at a working voltage of 100 kV. Samples (0.1 mg/mL or 1 mg/mL in methanol) were prepared using copper grids and 0.5% uranyl acetate stain. Fisher Scientific single syringe pump (95-120V/60Hz) was employed for controlled addition of PBS (pH 7.4) to prepare micellar solutions.

Synthesis and Experimental Procedures

Synthesis of 4–acryloyloxy–2–butanone (AB). 4–hydroxy–2–butanone (24 mL, 0.28 mol), triethylamine (78 mL, 0.56 mol, dried over molecular sieves), dichloromethane (DCM, 100 mL, dried over molecular sieves), and anhydrous sodium sulfate (20 g) were added to a 1000 mL round bottom flask equipped with a magnetic stir bar. The contents were allowed to cool below 5 °C while stirring in an acetone-ice bath. Acryloyl chloride (27.8 mL, 0.556 mol) was dissolved in dichloromethane (DCM, 100 mL) and added drop-wise through an addition funnel over 2 h. The temperature of the reaction mixture was maintained below 5 °C during addition. Stirring continued overnight at 25 °C, and the mixture was filtered under vacuum and washed with DCM several times. The filtrate was transferred to a separating funnel and washed with deionized water (×3), a saturated solution of sodium bicarbonate (×3), and brine (×3). The crude monomer was purified by flash chromatography using a gradient solvent composition of ethyl acetate/hexanes (15/85, 40/60, and 50/50 v/v). Yield: 10–15% in different batches. ^{1}H NMR (500 MHz, $CDCl_3$): δ = 6.25, 5.72 (dd each, 2H, vinyl –C$\underline{H}_2$), 5.97 (t, H, vinyl –C$\underline{H}$), 4.29 (t, 2H, –O–C$\underline{H}_2$–CH_2–), 2.70 (t, 2H), 2.08 (s, 3H). ^{13}C NMR (500 MHz, $CDCl_3$): δ = 130.9 ($\underline{C}H_2$=CH–), 127.9 (CH_2=$\underline{C}$H–), 165.9 (–CH$\underline{C}$OO–), 59.2 (–COO$\underline{C}H_2$–), 41.9 (–$\underline{C}H_2COCH_3$), 205.7(–$CH_2\underline{C}OCH_3$), 30.3(–CO$\underline{C}H_3$); HRMS^{+} $C_7H_{10}O_3$, Theoretical: 142.1530. Actual: 142.0582.

Synthesis of PDMA macro-chain-transfer agent (macroCTA) by RAFT polymerization of *N,N*–dimethylacrylamide. A typical procedure for the synthesis of PDMA macroCTA is as follows. DMA (14.43 g, 0.1456 mol), DMP (0.288 g, 0.786 mmol), AIBN (0.0065 g, 0.039 mmol), *s*-trioxane (0.355 g, 3.94 mmol), and 1,4–dioxane (16.5 mL) were sealed in a 50 mL round bottom flask with a rubber septum and purged with nitrogen for 40 min. The reaction flask was then placed on a preheated silicon oil bath at 60 °C. Samples were removed periodically by degassed syringe to determine monomer conversion by ^{1}H NMR spectroscopy. The polymerization was quenched after 2.6 h at 58% monomer conversion by removing the round bottom flask from the oil bath and opening it to expose its contents to atmospheric oxygen. The reaction solution was dialyzed in DI water through a regenerated cellulose dialysis tubing having molecular weight cut-off (MWCO) = 3.5 kg/mol, and the product was isolated by lyophilization resulting in poly(*N,N*–dimethylacrylamide) ($PDMA_{115}$ macroCTA, **P6**) ($M_{n,\ NMR}$ = 11,800 g/mol, and degree of polymerization (DP_n) = 115; $M_{n,SEC}$ = 10,700 g/mol; $M_{w,SEC\ MALS}$ = 11,000 g/mol and M_w/M_n = 1.10). A similar procedure was followed to prepare $PDMA_{110}$ (**P5**), $PDMA_{123}$ (**P7**), and $PDMA_{127}$ (**P8**).

RAFT polymerization of 4–acryloyloxy–2–butanone (AB) using $PDMA_{123}$ macroCTA ($PDMA_{123}$–*b*–PAB_{18}, P1). 4–Acryloyloxy–2–butanone (1.42 mL, 9.99 mmol), $PDMA_{123}$ macroCTA (2.5 g, 0.20 mmol), AIBN (0.003 g, 0.02 mmol), *s*–trioxane (0.09 g, 1 mmol), and 1,4–dioxane (7.5 mL) were sealed in a 20 mL vial with screw septa and purged with nitrogen for 30 min. The reaction vial was then placed on a preheated heating block at 70 °C. The reaction was quenched by removing the reaction vial from the heating block after 4.3 h at ~70% monomer conversion and opening to expose its contents to atmospheric oxygen. The reaction solution was precipitated in diethyl ether (×3) and dried under vacuum ($M_{n,NMR}$ = 15,100 g/mol and DP_n = 18; $M_{n,\ SEC}$ = 17,400 g/mol, M_w/M_n = 1.20).

Similar procedure was followed to prepare polymer **P3.**

RAFT polymerization of diacetone acrylamide using $PDMA_{115}$ macroCTA ($PDMA_{115}$–*b*–$PDAA_7$, P2). Diacetone acrylamide (1.31 g, 7.74 mmol), $PDMA_{115}$ macroCTA (3.02 g, 0.256 mmol), AIBN (0.0028 g, 0.017 mmol), *s*–trioxane (0.121 g, 1.34 mmol), and 1,4–dioxane (12 mL) were sealed in a 20 mL vial with screw septa and purged with nitrogen for 30 min. The reaction vial was then placed on a preheated heating block at 60 °C. The reaction was quenched by removing the vial from the heating block after 6 h at 45% monomer conversion and opening it to expose its contents to atmospheric oxygen. The reaction solution was dialyzed against deionized water. The reaction solution was dialyzed through a regenerated cellulose dialysis tubing (MWCO = 3.5 kg/mol) and the product was isolated by lyophilization resulting **$PDMA_{115}$–*b*–$PDAA_7$, P2** ($M_{n,NMR}$ = 13,500 g/mol; $M_{n,\ SEC}$ = 13,000 g/mol, $M_{w,MALS}$ = 13700 g/mol; M_w/M_n = 1.05).

Similar procedures were followed to prepare polymer **P4** and **P9–P12**.

Functionalization of $PDMA_{110}$–*b*–PAB_{37} (P3) with *O*–allyl hydroxylamine. $PDMA_{110}$–*b*–PAB_{37} (0.100 g, 0.223 mmol) was dissolved in THF (1 mL) in an 8 mL glass vial containing molecular sieves and a magnetic stir bar. *O*-Allyl hydroxylamine hydrochloride (0.049 g, 0.45 mmol) was dissolved in anhydrous THF (1 mL) along with TEA (186 µL, 1.34 mmol) and DI water (0.2 mL) and the resulting solution was added to the polymer solution under stirring. The reaction vial was kept under stirring at 25 °C for 6 h. The solution was then precipitated in cold hexane (×3), and dried under vacuum at 40 °C.

Functionalization of $PDMA_{110}$–*b*–PAB_{37} (P3) with *O*–(tetrahydro–2*H*–pyran–2–yl)hydroxylamine. $PDMA_{110}$–*b*–PAB_{37} (0.100 g, 0.223 mmol) was dissolved in THF (1 mL) in an 8 mL glass vial containing molecular sieves and magnetic stir bar. *O*–(Tetrahydro–2*H*–pyran–2–yl)hydroxylamine (0.053 g, 0.45 mmol) was dissolved in anhydrous THF (1 mL) and the resulting solution was added to the polymer solution under stirring. The reaction solution was continued to stir for 8 h at 25 °C. The solution was then precipitated in cold hexane (×3), and the product was dried under vacuum at 40 °C.

UV-Vis spectroscopy studies of the reaction of $PDMA_{127}$–*b*–$PDAA_{39}$ (P11) and *O*–(tetrahydro–2*H*–pyran–2–yl)hydroxylamine. Three solutions of $PDMA_{127}$–*b*–$PDAA_{39}$ (**P11**) (0.1 g, 0.2 mmol each) were prepared in methanol (3 mL

each) in three different 4 mL glass vials containing magnetic stir bars (solutions A, B, and C). A stock solution of *O*–(tetrahydro–2*H*–pyran–2–yl)hydroxylamine (0.10 g, 0.85 mmol) in methanol (1 mL) was added in two different portions (0.23 mL and 0.47 mL) to polymer solutions B and C. The mixed contents were stirred at 25 °C for 24 h. Solution A, without any added alkoxyamine, was used as the blank solution. The reactions were monitored periodically using UV-Vis spectroscopy by diluting the reaction solution aliquot (55 μL) with methanol (5 mL) before analysis.

UV-Vis spectroscopy studies of the reaction of DMP and *O*–(tetrahydro–2*H*–pyran–2–yl)hydroxylamine. Three solutions of DMP (0.020 g, 0.055 mmol each) were prepared in methanol (0.50 mL, 0.44 mL, 0.37 mL) in 4 mL glass vials containing magnetic stir bars (solutions A, B, and C respectively). A stock solution of *O*–(tetrahydro–2*H*–pyran–2–yl)hydroxylamine (0.05 g, 0.43 mmol) in methanol (0.5 mL) was added in two different portions (0.064 mL and 0.13 mL) to solutions B and C, respectively. The mixed contents were stirred at 25 °C for 24 h. Solution A, without any added alkoxyamine, was used as the blank solution. The reaction was monitored using UV-Vis spectroscopy by diluting the reaction solution aliquot (5 μL) with methanol (5 mL) before analysis.

Star formation and dissociation experiments with PDMA–*b*–PDAA.

Investigating the effect of the block copolymer concentration on star formation. To study the nature of the star formation in a selective solvent such that the block copolymers form micelles before cross linking, $PDMA_{127}$–*b*–$PDAA_7$ (**P9**) (0.400 g, 0.197 mmol) was dissolved in THF (5 mL) in a 40 mL vial. After complete dissolution, PBS (pH 7.4, 20 mL) was added at a rate of 9 mL/h using a syringe pump, and the resulting micellar solution was allowed to stir at 25 °C in an open vessel for 12 h. The solution was sonicated for 30 min, and the size of the micelles was determined using DLS.

O,O′–1,3–propanediylbishydroxylamine dihydrochloride (0.050 g, 0.28 mmol) was added to PBS (pH 7.4, 1 mL), and an aliquot of the resulting solution (0.710 mL) was transferred to the micellar solution under stirring to obtain a final $PDMA_{127}$–*b*–$PDAA_7$ concentration of 20 mg/mL. The reaction vial was kept at 25 °C under stirring and was monitored periodically using SEC, with the extent of star formation being calculated based on deconvolution via Gaussian multi peak fitting. The reaction solution was dialyzed through a regenerated cellulose dialysis tubing (MWCO = 50 kg/mol), and the product was isolated by lyophilization. Similarly the star formation was studied at [$PDMA_m$–*b*–$PDAA_n$] = 10 mg/mL and 20 mg/mL for other block copolymers (*m* = 127 and *n* = 7, 14, 39, 71).

Effect of [ketone]:[alkoxyamine] on star formation. A micellar solution of $PDMA_{127}$–*b*–$PDAA_{14}$ (**P10**) (0.24 g, 0.22 mmol) in PBS (pH 7.4, 12 mL) was prepared in a manner similar to that described above, and the solution (3 mL each) was transferred into four different 4 mL vials equipped with magnetic stir bars. *O,O′*–1,3–propanediylbishydroxylamine dihydrochloride (0.050 g, 0.28 mmol) was added to PBS (pH 7.4, 1 mL) and aliquots (0.097 mL, 0.20 mL, 0.39 mL, and 0.59 mL) of the resulting solution were added to the four different vials containing the micellar solution under stirring to obtain final $PDMA_{127}$–*b*–$PDAA_{14}$ concentration of 20 mg/mL. The reaction vials were kept at 25 °C under stirring and were monitored periodically using SEC, with the extent of star formation being calculated based on the Gaussian multi peak fitting. The reaction solutions were dialyzed with regenerated cellulose dialysis tubing (MWCO = 50 kg/mol), and the products were isolated by lyophilization.

Kinetics of star formation with $PDMA_m$–*b*–$PDAA_n$. To study the kinetics of the star formation in an aqueous system, micellar solutions of $PDMA_m$–*b*–$PDAA_n$ (10 mg/mL and 20 mg/mL) were prepared in PBS (pH 7.4) in a manner similar to that described before. The sizes of the micelles were determined by DLS. The kinetics of star formation were studied at polymer concentrations of 10 mg/mL and 20 mg/mL, and stoichiometries of [ketone]:[alkoxyamine] = 1:1 and 1:2 for various block copolymers ($PDMA_m$–*b*–$PDAA_n$; *m* = 127 and *n* = 7, 14, 39, 71). *O,O′*–1,3–propanediylbishydroxylamine dihydrochloride (0.050 g, 0.28 mmol) was added to PBS (pH 7.4, 1 mL) and aliquots (0.0530 mL, 0.106 mL) of were added to two different vials containing micellar solutions of $PDMA_{127}$–*b*–$PDAA_7$ (3 mL, 10 mg/mL; 3 mL, 20 mg/mL, respectively) under stirring. The mixed contents were stirred at 25 °C, and the reaction progress was monitored periodically using SEC. The kinetics of star formation were studied in a similar method for other block copolymers $PDMA_m$–*b*–$PDAA_n$ (*m* = 127 and *n* = 7, 14, 39, 71).

Kinetics of star formation with $PDMA_m$–*b*–$PDAA_n$ in a non-selective solvent. To study the kinetics of the star formation in a non-selective solvent, $PDMA_{127}$–*b*–$PDAA_{14}$ (0.09 g, 0.08 mmol) was dissolved in MeOH (1.2 mL) in a 4 mL vial equipped with a stir bar. *O,O′*–1,3–propanediylbishydroxylamine dihydrochloride (0.050 g, 0.28 mmol) was added to a mixture of MeOH (0.9 mL) and TEA (0.078 mL, 0.56 mmol) under stirring. An aliquot (0.30 mL) of the resulting solution was added to the polymer solution under stirring to obtain the final $PDMA_{127}$–*b*–$PDAA_{14}$ concentration of 60 mg/mL. The reaction vial was kept at 25 °C under stirring and the reaction progress was monitored periodically using SEC, with the extent of star formation being calculated based on deconvolution via Gaussian multi peak fitting. The reaction solution was dialyzed with a regenerated cellulose dialysis tubing (MWCO = 50 kg/mol) and the product was isolated by lyophilization.

Kinetics of Oxime Star Dissociation. Star dissociation experiments were carried out using furfuraldehyde, acetone, and *O*–allyl hydroxylamine hydrochloride.

Star dissociation with monofunctional alkoxyamine: Purified oxime stars (**Star 2)** (0.010 g, 0.015 mmol) was dissolved in PBS (pH 7.4, 1.0 mL) in a 4 mL vial containing a magnetic stir bar. A solution of *O*–allyl hydroxylamine hydrochloride (0.084 g, 0.77 mmol) in PBS (0.84 mL) was added to the star solution along with trifluroacetic acid (TFA, 60 μL). The reaction vial was kept

on preheated hot plate at 60 °C under stirring. The progress of the reaction was monitored periodically by SEC. An aliquot of the reaction solution (60 µL) was diluted with methanol (1 mL) prior to analysis by DLS.

Star degradation with furfuraldehyde: Purified oxime stars (**Star 12)** (0.0153 g, 0.0920 mmol) was dissolved in PBS (pH 7.4, 1.5 mL), and furfuraldehyde (0.38 mL, 0.0046 mol) was added to this solution along with TFA (10 µL). The reaction vial was kept on a preheated hot plate at 60 °C under stirring. The progress of the reaction was monitored periodically by SEC. An aliquot of the reaction solution (60 µL) was diluted with methanol (1 mL) prior to analysis by DLS.

Star degradation study with acetone was performed in a similar manner.

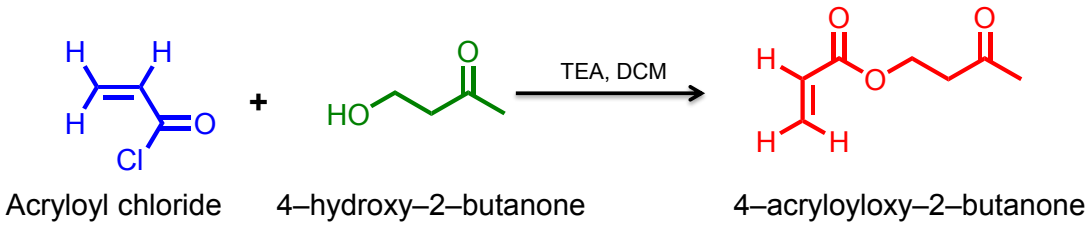

Scheme S1. Synthesis of 4–acryloyloxy 2–butanone (AB).

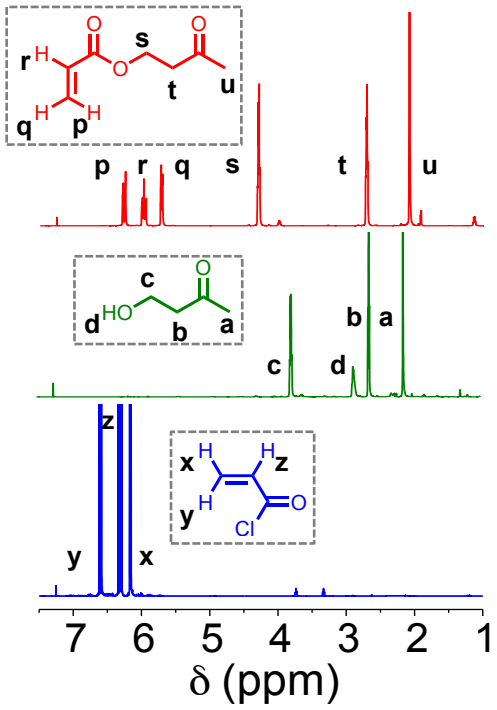

Fig. S1. ^{1}H NMR spectra of acryloyl choride, 4–hydroxy–2–butanone, and 4–acryloyloxy–2–butanone in $CDCl_3$.

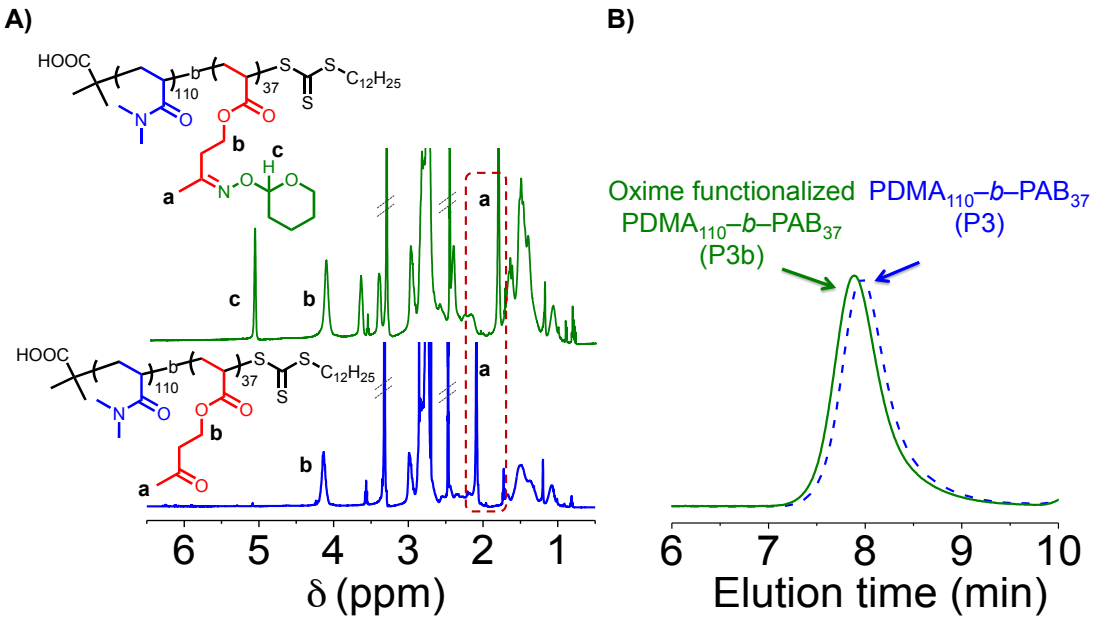

Fig. S2. Functionalization of $PDMA_{110}$–*b*–PAB_{37} (**P3**) with *O*–(tetrahydro–2*H*–pyran–2–yl)hydroxylamine (A) ^{1}H NMR spectra of $PDMA_{110}$–*b*–$PDAA_{37}$ before (blue) and after functionalization (green) in DMSO–d_6. (B) Overlay SEC refractive index traces of $PDMA_{110}$–*b*–$PDAA_{37}$ (**P3**) and functionalized $PDMA_{110}$–*b*–$PDAA_{37}$ (**P3b**).

Table S1. Results for Functionalization of $PDMA_{110}$–*b*–PAB_{37} with Monofunctional Alkoxyamines

Polymer	**Monofunctional alkoxyamine used**	**[ketone] : [alkoxyamine]**	**% Functionalization**	**$M_{n,\,NMR}$ (g/mol) of functionalized polymers**
$PDMA_{110}$–*b*–PAB_{37} (**P3**)	*O*–allyl hydroxyl amine hydrochloride	1 : 2	99	17,800 (**P3a**)
$PDMA_{110}$–*b*–PAB_{37} (**P3**)	*O*–(tetrahydro–2*H*–pyran–2–yl) hydroxylamine	1 : 2	99	18,800 (**P3b**)

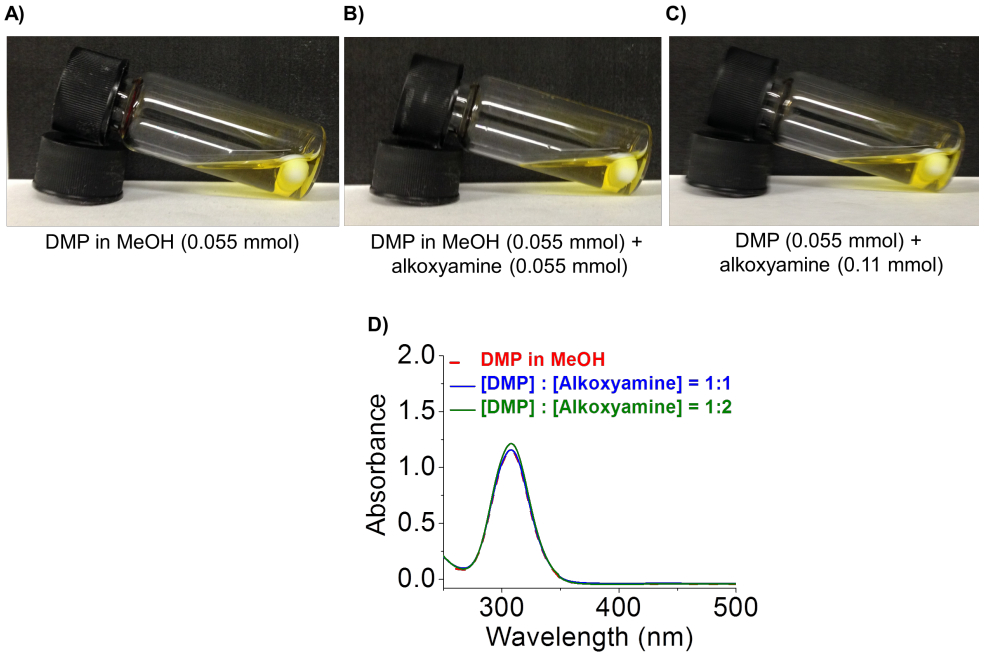

Fig. S3. Photographs of (A) solution of 2–dodecylsulfanylthiocarbonylsulfanyl–2–methyl–propionic acid (DMP) in methanol, (B) reaction solution of DMP with 1 equiv of *O*–(tetrahydropyran–2*H*–pyran–2–yl)hydroxylamine in methanol, and (C) reaction solution of DMP with 2 equiv of *O*–(tetrahydropyran–2*H*–pyran–2–yl)hydroxylamine in methanol after 24 h at 25 °C. (D) UV-Vis spectra of DMP in MeOH before and after the reaction with *O*–(tetrahydro–2*H*–pyran–2–yl)hydroxylamine.

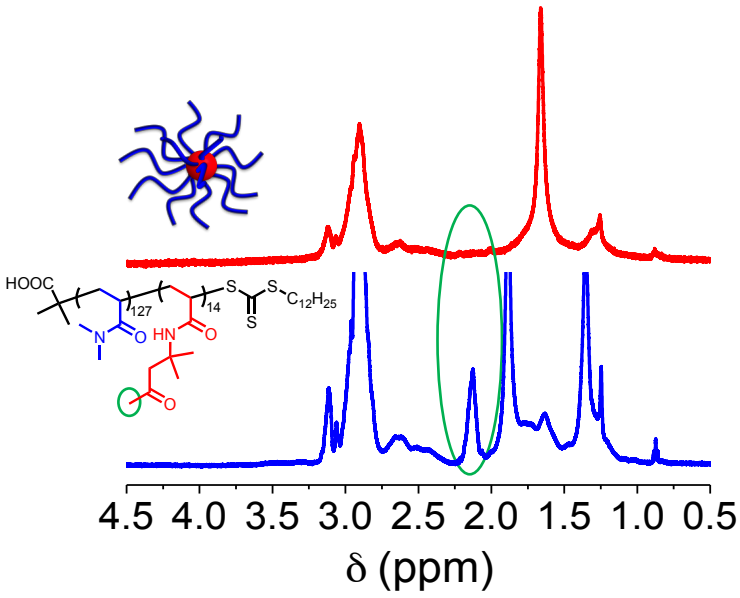

Fig. S4. ^{1}H NMR spectra of core-crosslinked oxime stars (**Star 1**, red) and $PDMA_{127}$–*b*–$PDAA_{14}$ (**P10**, blue) in $CDCl_3$.

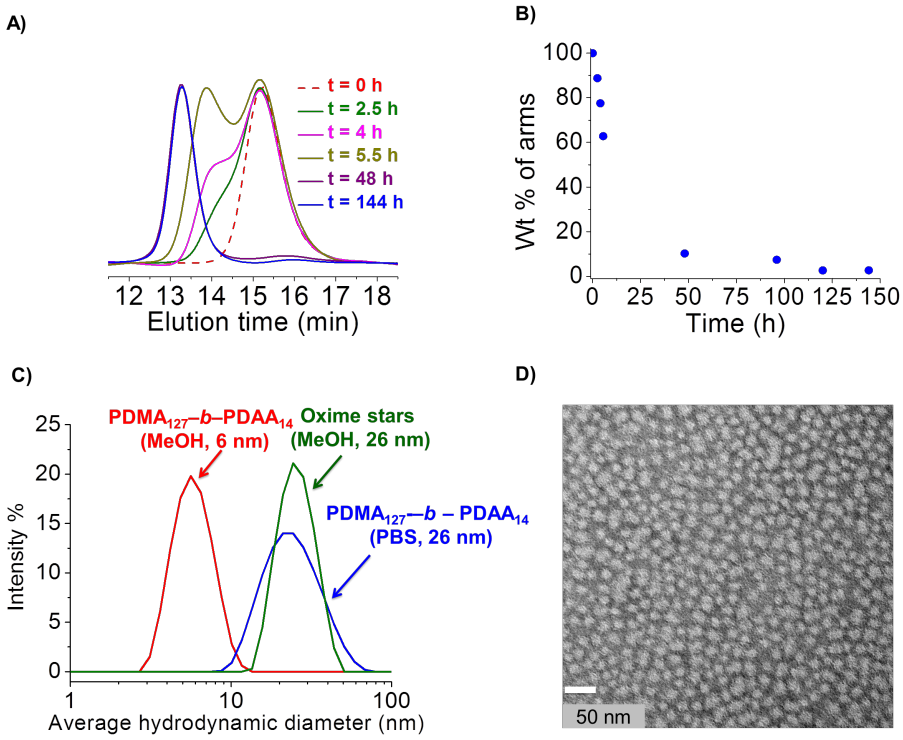

Fig. S5. (A) Normalized refractive index SEC traces showing progress of star (**Star 2**) formation reaction and (B) kinetics of star formation determined by deconvolution of refractive index SEC traces obtained during the reaction between $PDMA_{127}$–*b*–$PDAA_{14}$ (**P10,** 20 mg/mL) and *O,O'*–1,3–propanediylbishydroxylamine in PBS at [ketone]:[alkoxyamines] = 1:2 equiv. (C) DLS solution size distribution for $PDMA_{127}$–*b*–$PDAA_{14}$ in MeOH (red), as micelles formed in PBS (blue), and as purified core-crosslinked oxime stars in MeOH (green). (D) TEM image of purified core-crosslinked oxime stars in MeOH (negative stained, white scale bar: 50 nm).

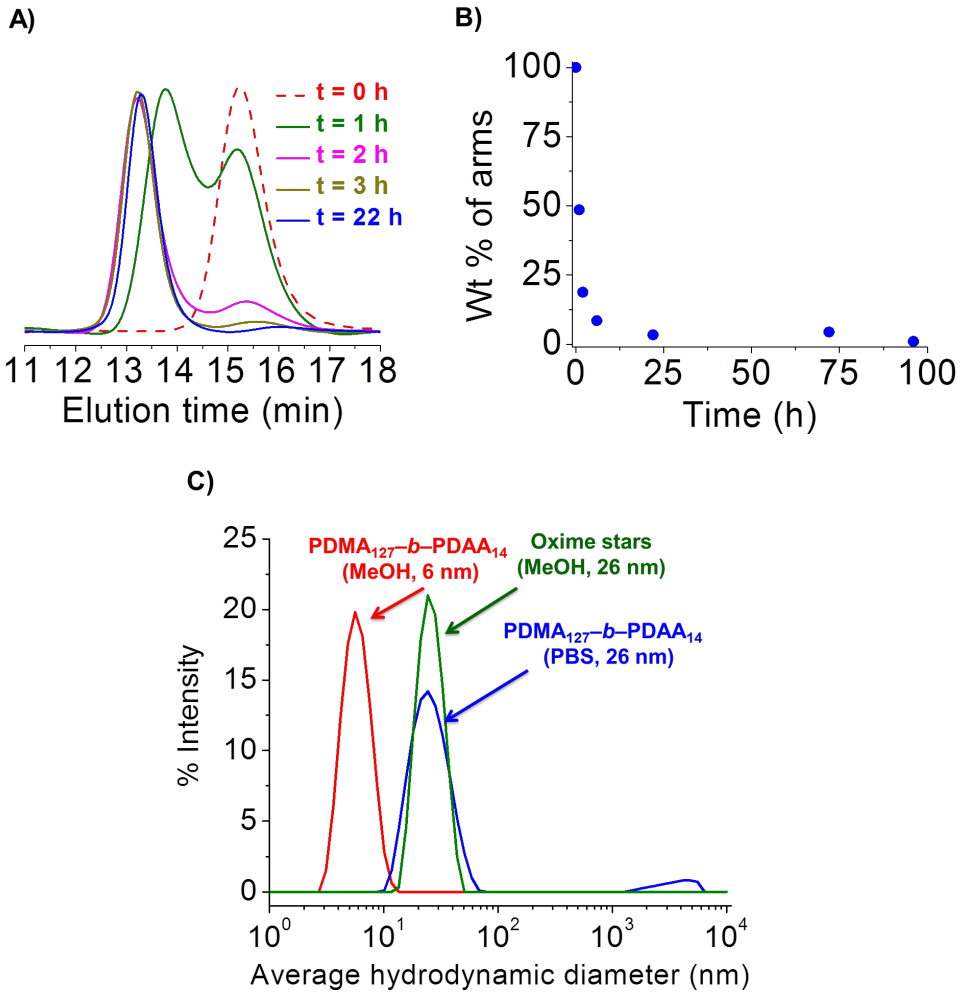

Fig. S6. (A) Normalized refractive index SEC traces showing progress of star (**Star 3**) formation reaction and (B) kinetics of star formation determined by deconvolution of refractive index SEC traces obtained during the reaction between $PDMA_{127}$–*b*–$PDAA_{14}$ (**P10,** 20 mg/mL) and *O,O'*–1,3–propanediylbishydroxylamine in PBS at [ketone]:[alkoxyamines] = 1:4 equiv. (C) DLS solution size distribution for $PDMA_{127}$–*b*–$PDAA_{14}$ in MeOH (red), as micelles formed in PBS (blue), and as purified core-crosslinked oxime stars in MeOH (green).

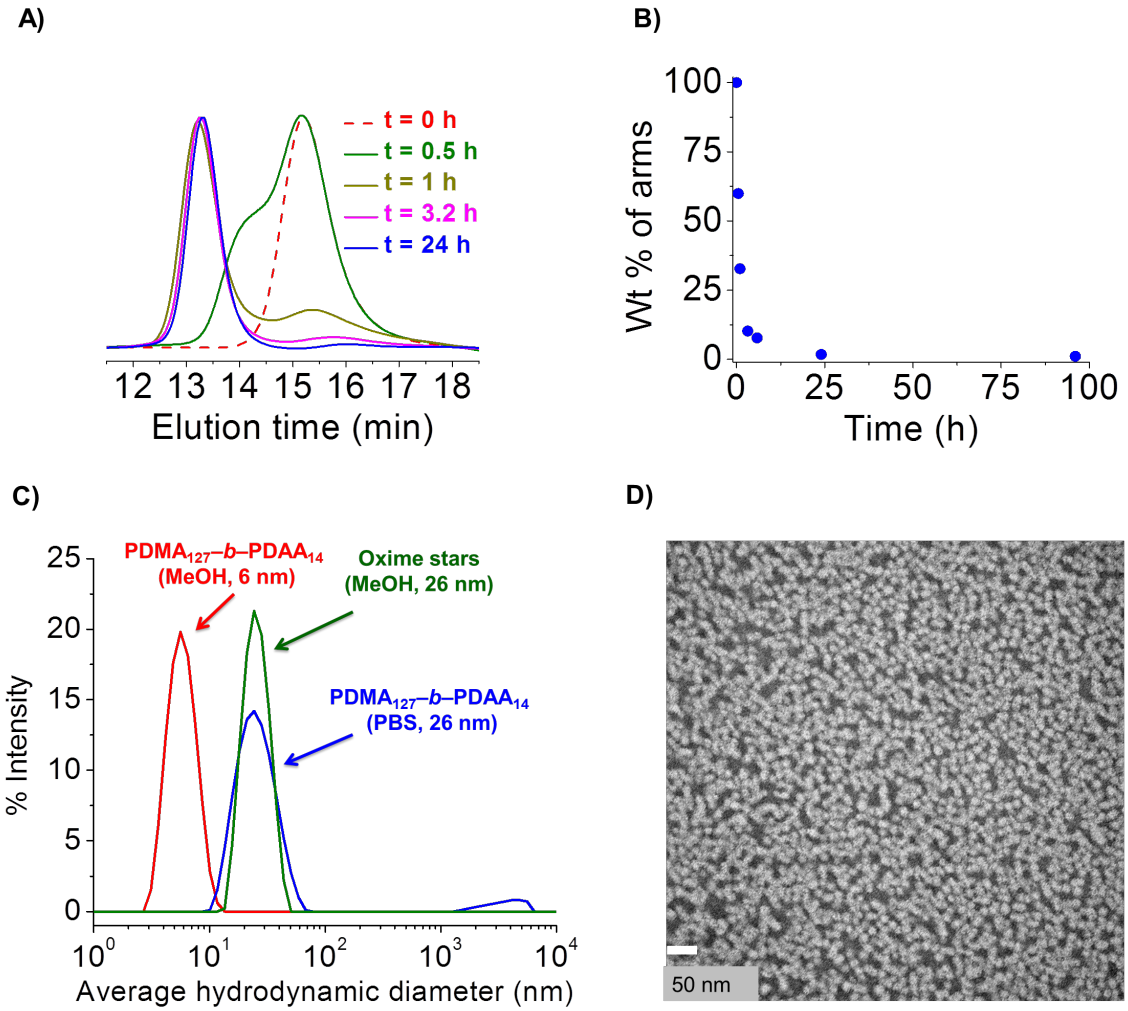

Fig. S7. (A) Normalized refractive index SEC traces showing progress of star (**Star 4**) formation reaction and (B) kinetics of star formation determined by deconvolution of refractive index SEC traces obtained during the reaction between $PDMA_{127}$–*b*–$PDAA_{14}$ (**P10,** 20 mg/mL) and *O,O'*–1,3–propanediylbishydroxylamine in PBS at [ketone]:[alkoxyamines] = 1:6 equiv. (C) DLS solution size distribution of $PDMA_{127}$–*b*–$PDAA_{14}$ (red), as micelles formed in PBS (blue), and as purified core-crosslinked oxime stars (green).(D) TEM image of purified core-crosslinked oxime stars (negative stain, white scale bar: 50 nm).

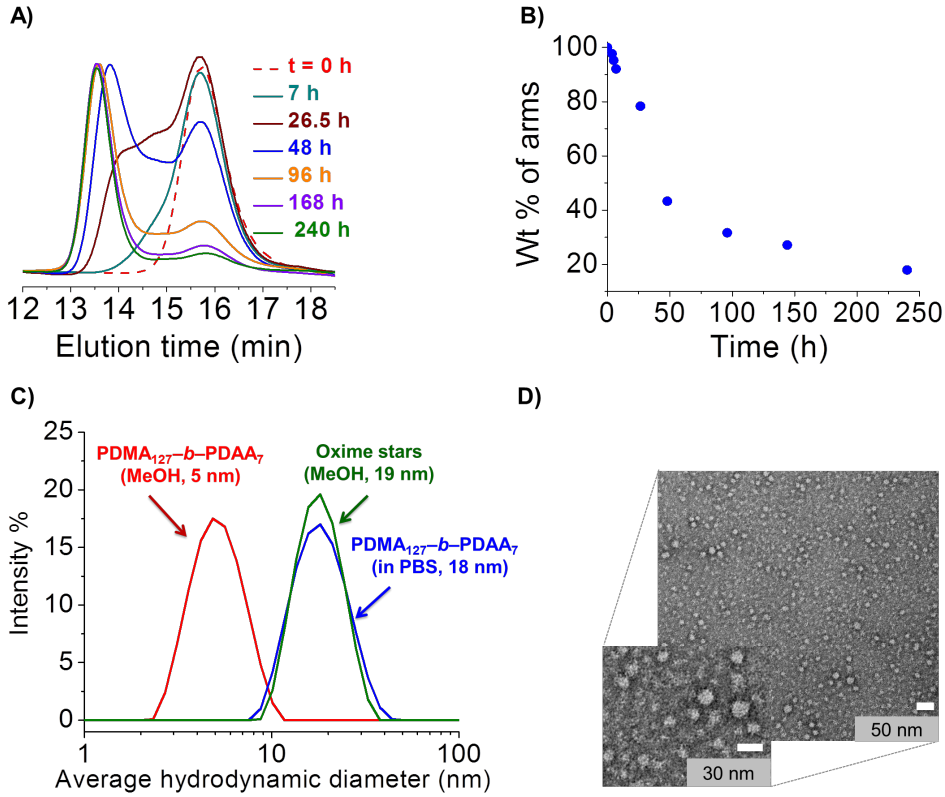

Fig. S8. (A) Normalized refractive index SEC traces showing progress of star (**Star 5**) formation reaction and (B) kinetics of star formation determined by deconvolution of refractive index SEC traces obtained during the reaction between $PDMA_{127}$–*b*–$PDAA_7$ (**P9,** 10 mg/mL) and *O,O′*–1,3–propanediylbishydroxylamine in PBS at [ketone]:[alkoxyamines] = 1:2 equiv. (C) DLS solution size distribution of $PDMA_{127}$–*b*–$PDAA_7$ in MeOH (red), as micelles formed in PBS (blue), and as purified core-crosslinked oxime stars in MeOH (green). (D) TEM image of purified core-crosslinked oxime stars (white scale bars: 30 nm (inset) and 50 nm).

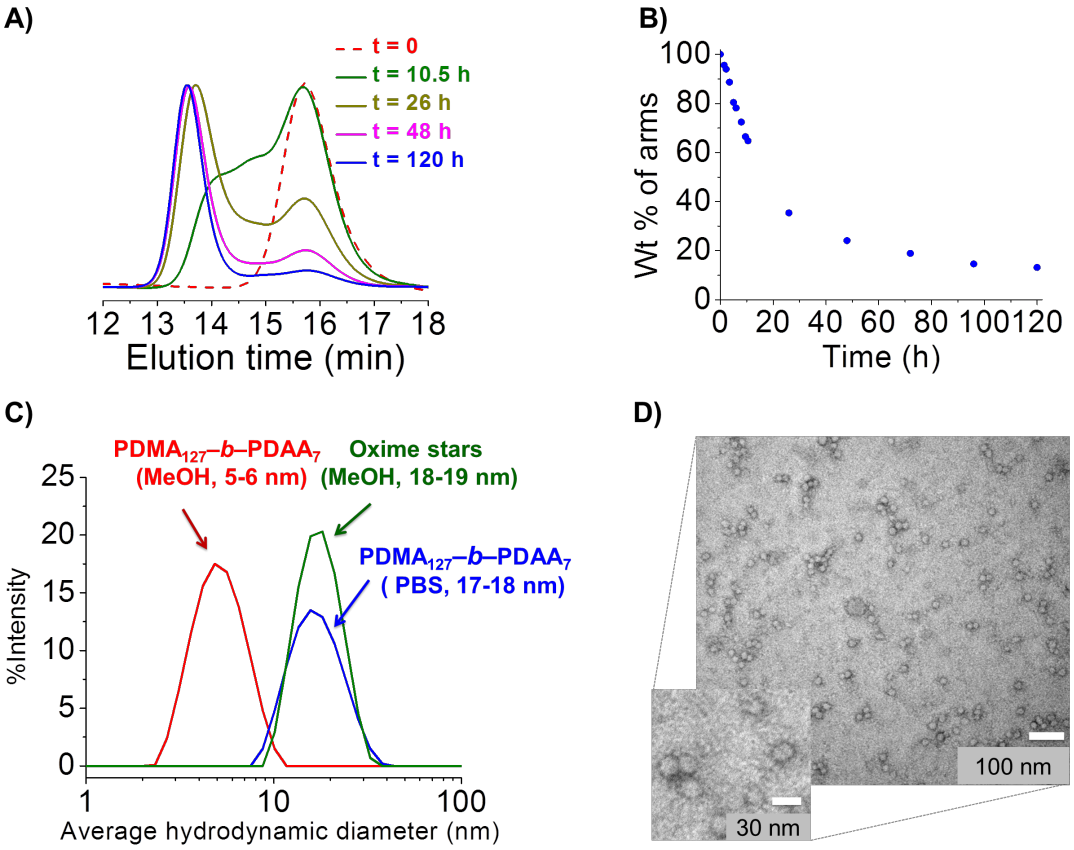

Fig. S9. (A) Normalized refractive index SEC traces showing progress of star (**Star 6**) formation reaction and (B) kinetics of star formation determined by deconvolution of refractive index SEC traces obtained during the reaction between $PDMA_{127}$–*b*–$PDAA_7$ (**P9,** 20 mg/mL) and *O,O'*–1,3–propanediylbishydroxylamine in PBS at [ketone]:[alkoxyamines] = 1:2 equiv. (C) DLS solution size distribution of $PDMA_{127}$–*b*–$PDAA_7$ in MeOH (red), as micelles formed in PBS (blue), and as purified core-crosslinked oxime stars in MeOH (green). (D) TEM image of purified core-crosslinked oxime stars (negative stain, white scale bars: 30 nm (inset) and 100 nm).

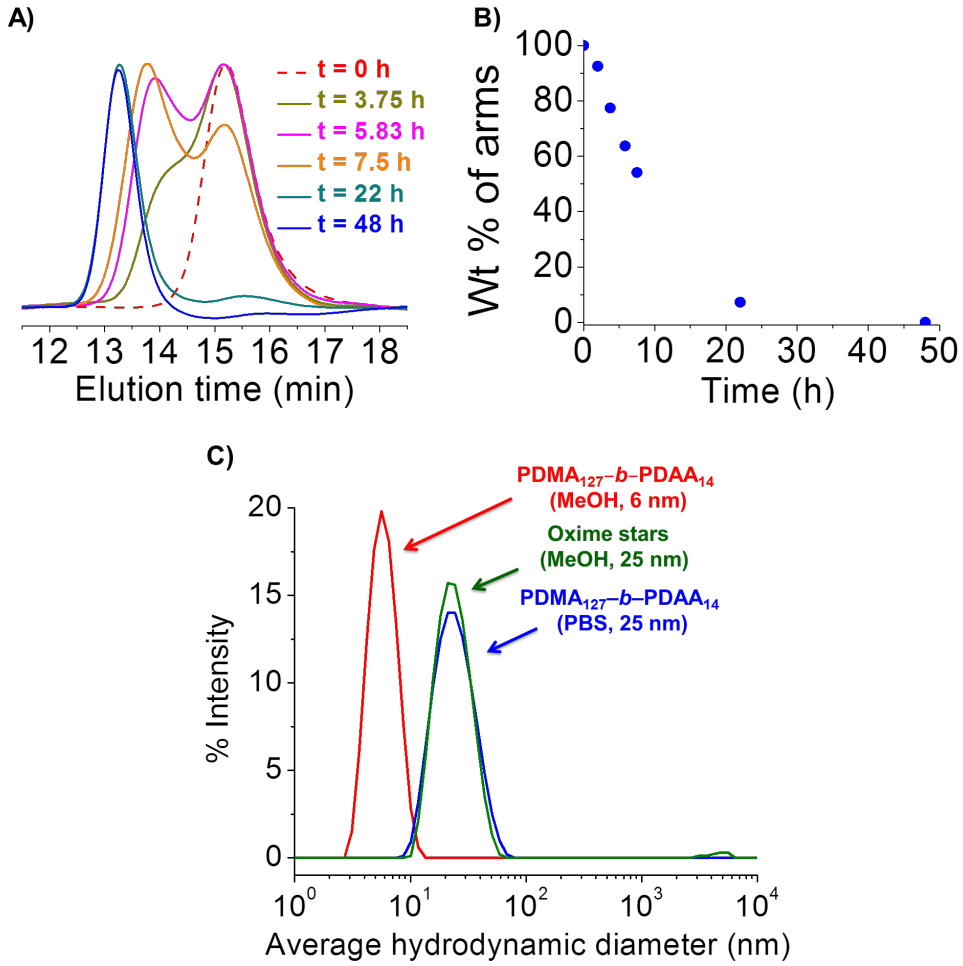

Fig. S10. (A) Normalized refractive index SEC traces showing progress of star (**Star 7**) formation reaction and (B) kinetics of star formation determined by deconvolution of refractive index SEC traces obtained during the reaction between $PDMA_{127}$–*b*–$PDAA_{14}$ (**P10,** 10 mg/mL) and *O,O'*–1,3–propanediylbishydroxylamine in PBS at [ketone]:[alkoxyamines] = 1:2 equiv. (C) DLS solution size distribution of $PDMA_{127}$–*b*–$PDAA_{14}$ in MeOH (red), as micelles formed in PBS (blue), and as purified core-crosslinked oxime stars in MeOH (green).

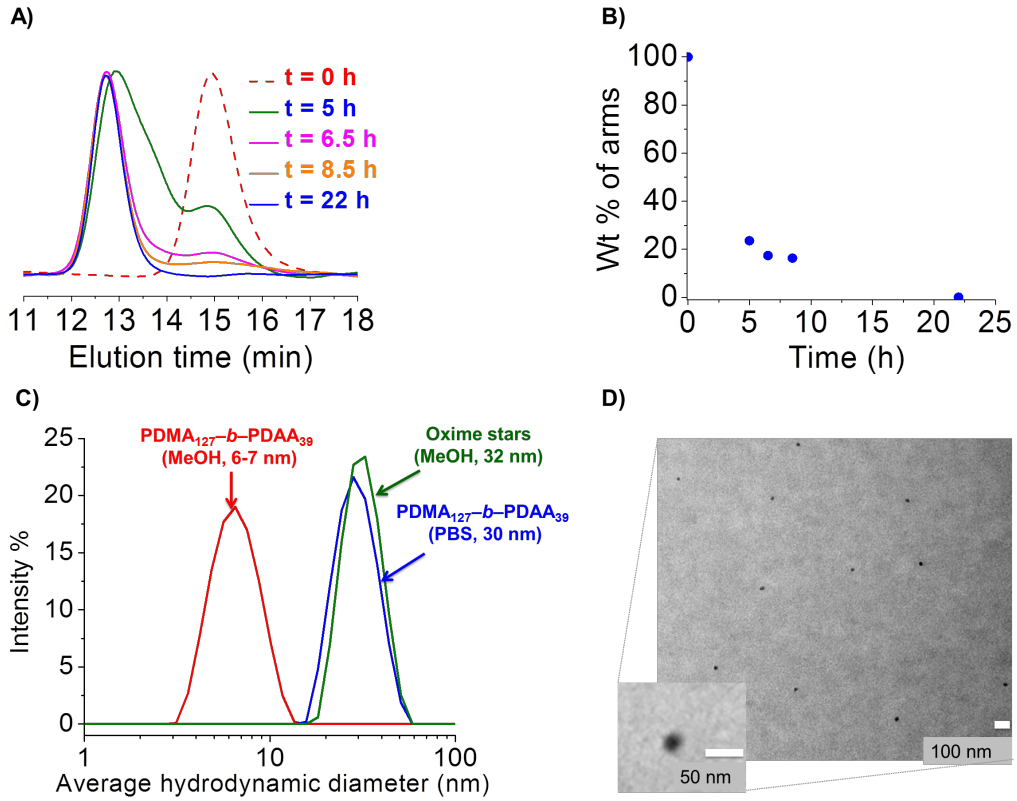

Fig. S11. (A) Normalized refractive index SEC traces showing progress of star (**Star 8**) formation reaction and (B) kinetics of star formation determined by deconvolution of refractive index SEC traces obtained during the reaction between $PDMA_{127}$–*b*–$PDAA_{39}$ (**P11,** 10 mg/mL) and *O,O'*–1,3–propanediylbishydroxylamine in PBS at [ketone]:[alkoxyamines] = 1:2 equiv. (C) DLS solution size distribution of $PDMA_{127}$–*b*–$PDAA_{39}$ in MeOH (red), as micelles formed in PBS (blue), and as purified core-crosslinked oxime stars in MeOH (green). (D) TEM image of purified core-crosslinked oxime stars (white scale bars: 50 nm (inset) and 100 nm).

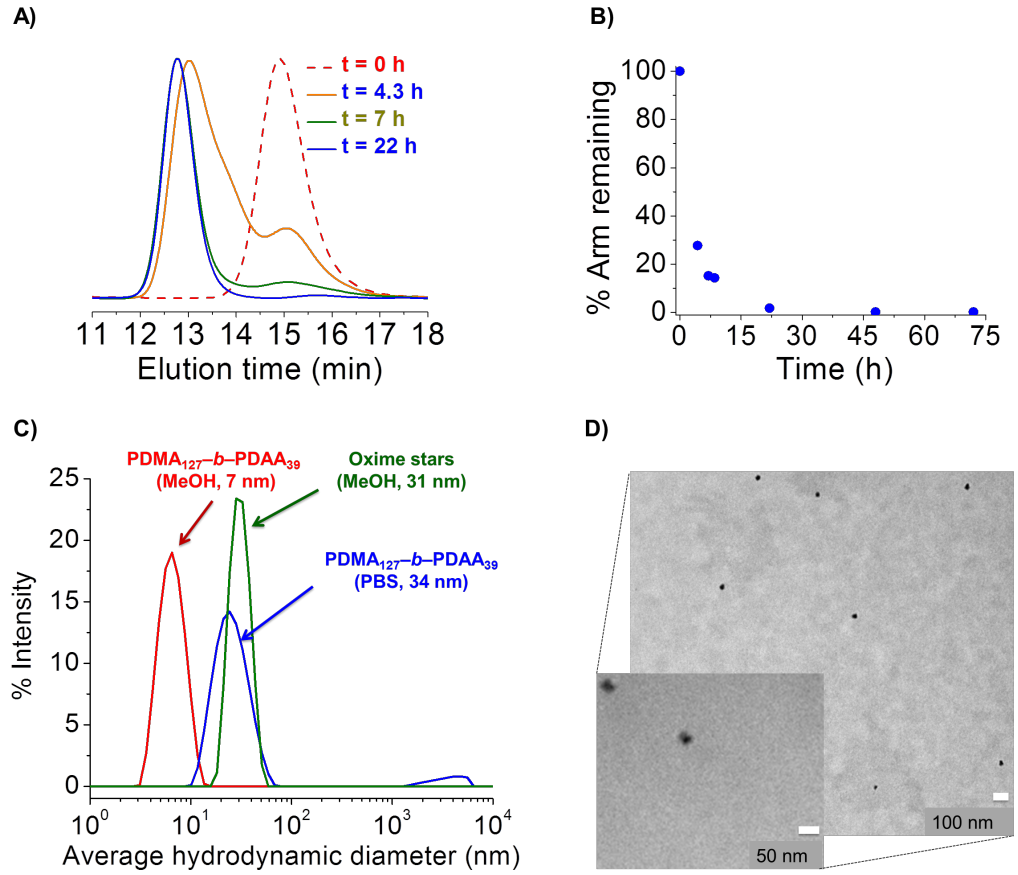

Fig. S12. (A) Normalized refractive index SEC traces showing progress of star (**Star 9**) formation reaction and (B) kinetics of star formation determined by deconvolution of refractive index SEC traces obtained during the reaction between $PDMA_{127}$–*b*–$PDAA_{39}$ (**P11,** 20 mg/mL) and *O,O'*–1,3–propanediylbishydroxylamine in PBS at [ketone]:[alkoxyamines] = 1:2 equiv. (C) DLS solution size distribution of $PDMA_{127}$–*b*–$PDAA_{39}$ in MeOH (red), as micelles formed in PBS (blue), and as purified core-crosslinked oxime stars in MeOH (green). (D) TEM image of purified core-crosslinked oxime stars (white scale bars: 50 nm and 100 nm).

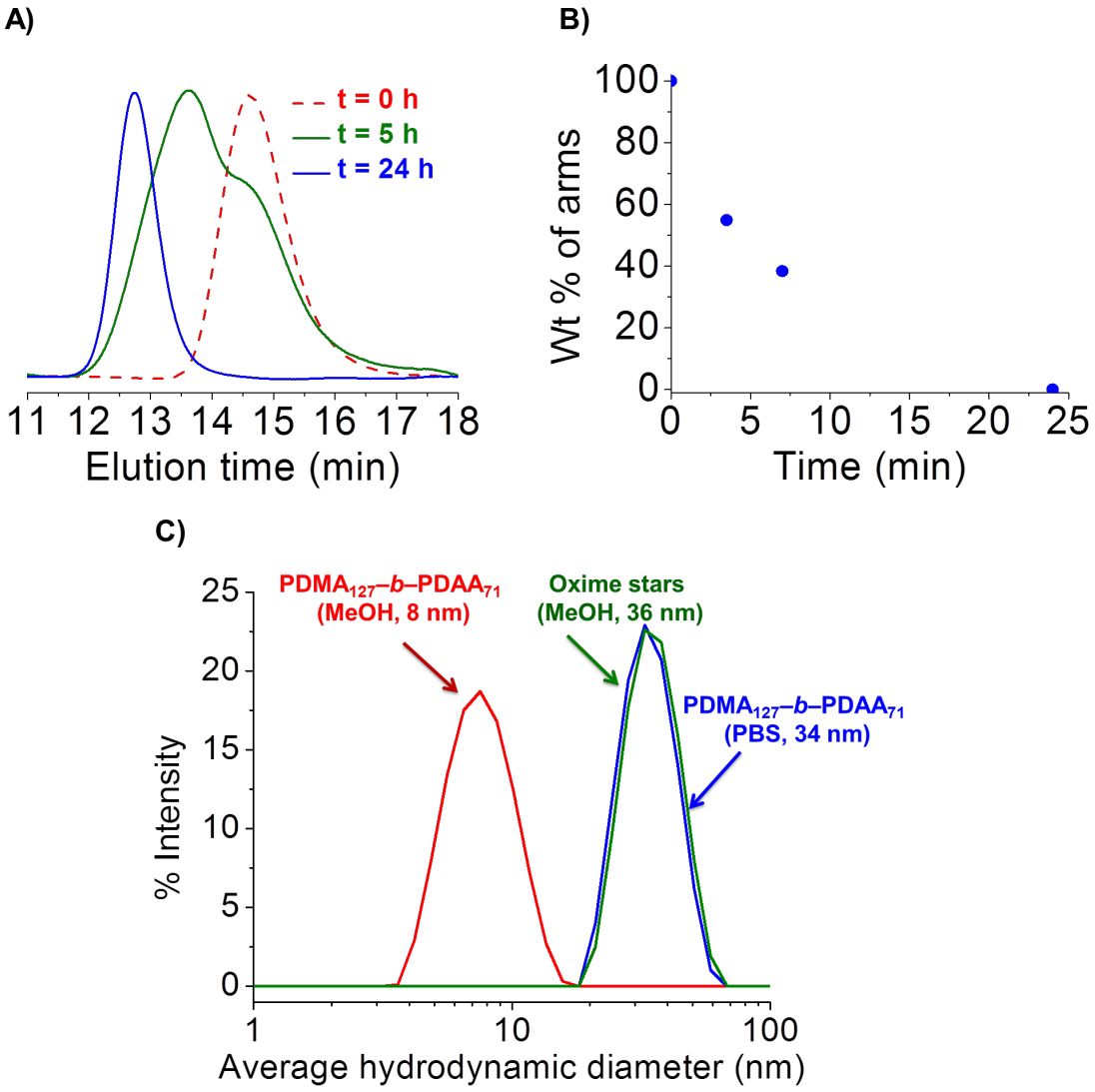

Fig. S13. (A) Normalized refractive index SEC traces showing progress of star (**Star 10**) formation reaction and (B) kinetics of star formation determined by deconvolution of refractive index SEC traces obtained during the reaction between $PDMA_{127}$–*b*–$PDAA_{71}$ (**P12,** 10 mg/mL) and *O,O'*–1,3–propanediylbishydroxylamine in PBS at [ketone]:[alkoxyamines] = 1:2 equiv. (C) DLS solution size distribution of $PDMA_{127}$–*b*–$PDAA_{71}$ in MeOH (red), as micelles formed in PBS (blue), and as purified core-crosslinked oxime stars in MeOH (green).

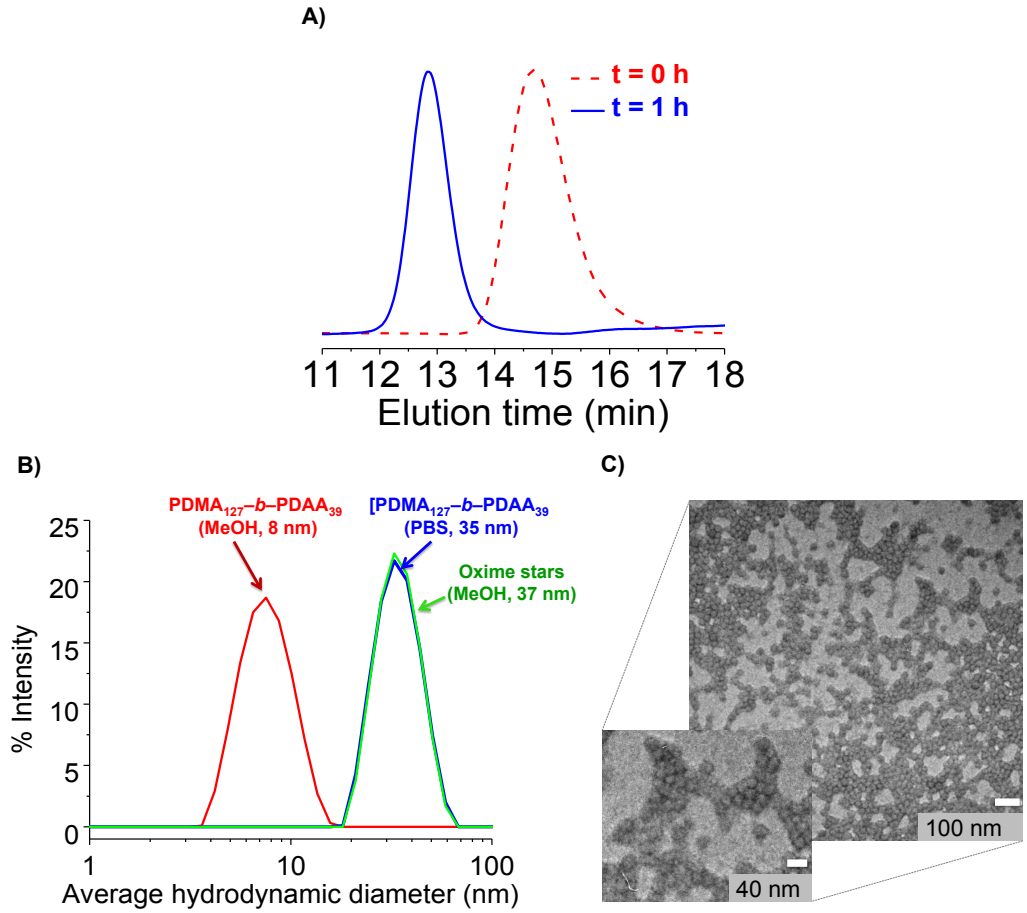

Fig. S14. (A) Normalized refractive index SEC traces showing progress of star (**Star 11**) formation reaction between $PDMA_{127}$–*b*–$PDAA_{71}$ (**P12,** 20 mg/mL) and *O,O'*–1,3–propanediylbishydroxylamine in PBS at [ketone]:[alkoxyamines] = 1:2 equiv. (B) DLS solution size distribution of $PDMA_{127}$–*b*–$PDAA_{71}$ in MeOH (red), as micelles formed in PBS (blue), and as purified core-crosslinked oxime stars in MeOH (green). (C) TEM image of purified core-crosslinked oxime stars (negative stained, white scale bar: 40 nm (unset) and 100 nm).

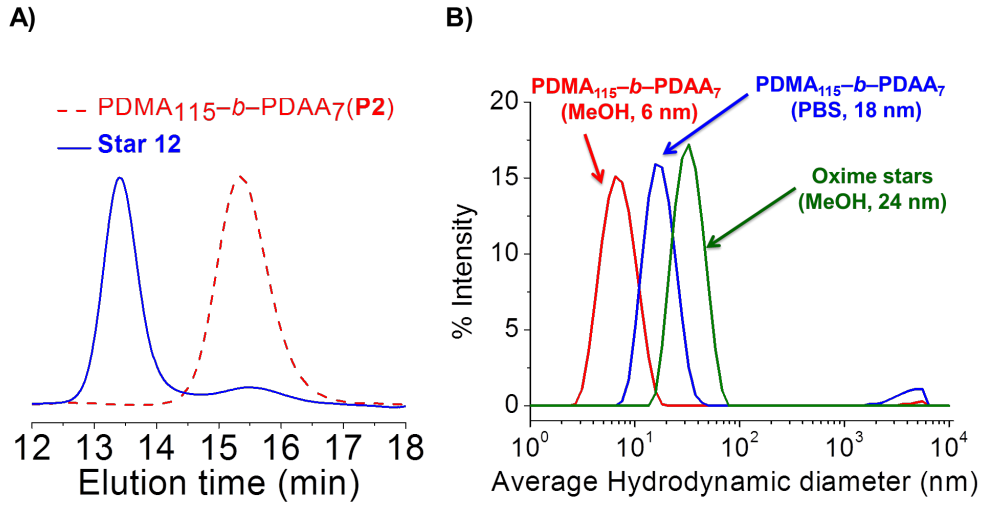

Fig. S15. (A) Overlay of normalized refractive index SEC traces of $PDMA_{115}$–*b*–$PDAA_7$ and purified oxime stars (**Star 12**) formed by the reaction between $PDMA_{115}$–*b*–$PDAA_7$ (**P2,** 20 mg/mL) and *O,O'*–1,3–propanediylbishydroxylamine at [ketone]:[alkoxyamine] = 1:2 equiv in PBS. (B) DLS solution size distribution of $PDMA_{115}$–*b*–$PDAA_7$ in MeOH (red), as micelles formed in PBS (blue), and as purified core-crosslinked oxime stars in MeOH (green).

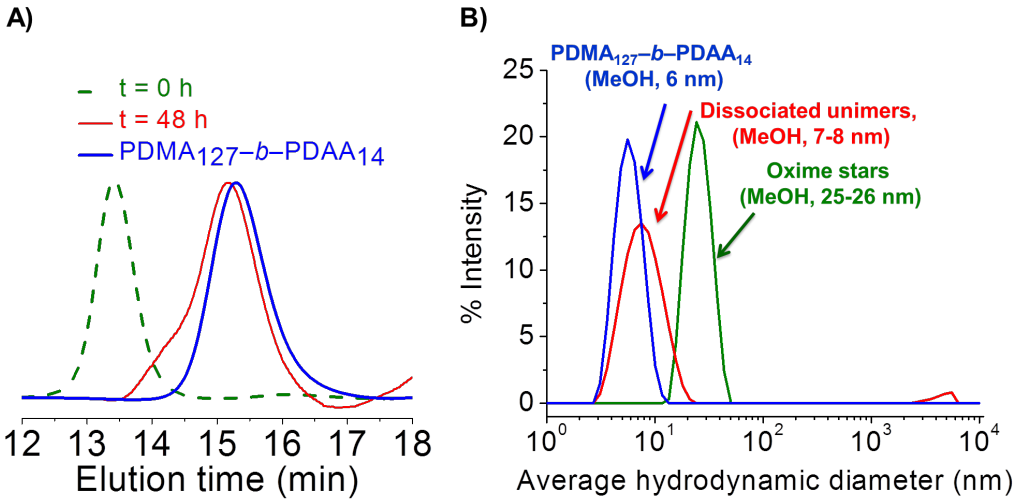

Fig. S16. (A) Normalized refractive index SEC traces of purified oxime star (**Star 2**, green), dissociated unimers (red) after 48 h of reaction between oxime stars and *O*–allyl hydroxylamine in presence of TFA at 60 °C, and $PDMA_{127}$–*b*–$PDAA_{14}$ (**P10**, blue). (B) DLS solution size distribution of $PDMA_{127}$–*b*–PAB_{14} in MeOH (blue), dissociated unimers in MeOH (red), and purified core-crosslinked oxime stars in MeOH (green).

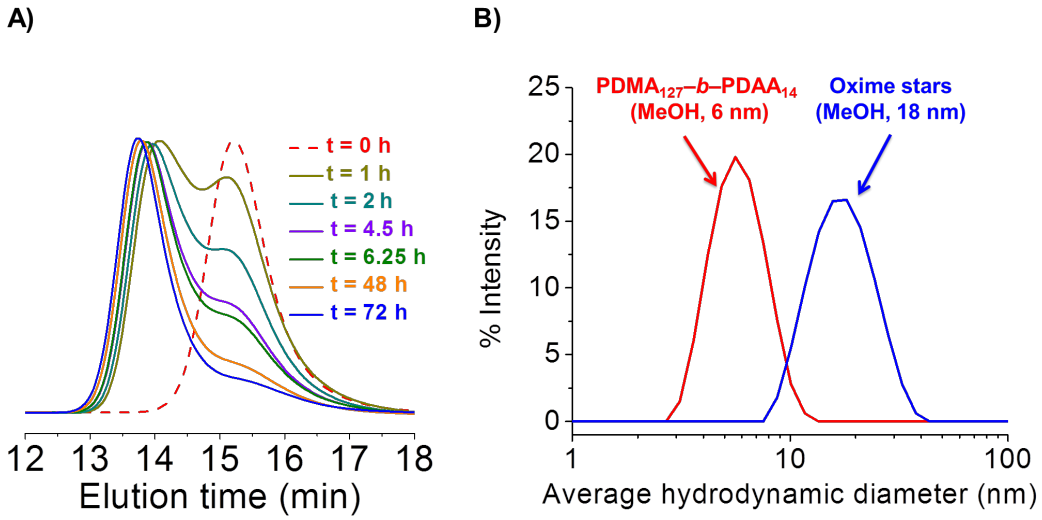

Fig. S17. (A) Normalized SEC refractive index traces showing progress of star formation reaction between $PDMA_{127}$–*b*–$PDAA_{14}$ (**P10, 6**0 mg/mL) and *O,O'*–1,3–propanediylbishydroxylamine at [ketone]:[alkoxyamine] = 1:2 equiv in MeOH. (B) DLS solution size distribution of $PDMA_{127}$–*b*–$PDAA_{14}$ in MeOH (red) and as core-crosslinked oxime stars in MeOH (blue).

References

(1) Lai, J. T.; Filla, D.; Shea, R. *Macromolecules* 2002, *35*, 6754.